Note: Extraction of Compton Form Factors with combined fits of Spacelike and Timelike Deeply Virtual Compton Scattering

Marie Boër,*
Temple University, Philadelphia, PA, USA.

December, 2018

Abstract

Deeply Virtual Compton Scattering (DVCS) and Timelike Compton Scattering (TCS) consist of the scattering of photons off a quark in the nucleon. These reactions are sensitive to the Generalized Parton Distribution (GPDs) which contain the information on the transverse position and on the longitudinal momentum distributions of the quarks. The GPD functions actually extractable from experiments are the Compton Form Factors (CFFs), which are integrals of GPDs ot the GPDs at specific point. In this note, we report on the simulations that we have carried out to estimate with which sensitivity one can extract the CFFs from experimental data from the combined or separate analysis of various DVCS and TCS observables. Our work is done for typical Jefferson Lab. 12 GeV kinematics, where several DVCS and TCS experiments are planned in the near future.

1 Introduction

Generalized Parton Distributions (GPDs) contain the correlation between the spatial transverse distribution of partons and the longitudinal momentum in the nucleon. GPDs depend at leading order on 3 variables: x which is the longitudinal momentum fraction of nucleon's momentum carried by the parton, ξ which is the longitudinal momentum transfer to the parton, and t which is the square 4-momentum transfer to the nucleon. "Spacelike" Deeply Virtual Compton Scattering (DVCS = $eN \hookrightarrow \gamma^* N \rightarrow e'N'\gamma$ - Fig. 1) and Timelike Compton Scattering (TCS = $\gamma N \hookrightarrow \gamma^* N' \rightarrow e^+e^-N'$ - Fig. 2) are two processes accessing GPDs of the nucleon. DVCS corresponds to the leptoproduction of a real photon and TCS to the photoproduction of a lepton pair. In the following we will consider only electrons for leptons, i.e. electroproduction for DVCS and electron-positron pair production for TCS. Taking massless quarks and at leading order of QCD (Quantum Chromodynamics), the two processes depend on 4 GPDs for the nucleon, H, E, $\tilde{\text{H}}$, $\tilde{\text{E}}$, corresponding to study independent relative polarizations of the photons and the quarks. We restrict our study in the present note to quark GPDs and to the proton. The GPD dependence of the reaction amplitudes is contained in Compton Form Factors (CFFs), which are complex functions

*contact: mboer@jlab.org

of GPDs. In this note, our notation for the CFFs associated to GPDs is the following:

$$H_{Re}(\xi,t) \equiv \mathcal{P}\int_0^1 dx\,[H(x,\xi,t) - H(-x,\xi,t)]\,C^+(x,\xi), \quad (1)$$

$$E_{Re}(\xi,t) \equiv \mathcal{P}\int_0^1 dx\,[E(x,\xi,t) - E(-x,\xi,t)]\,C^+(x,\xi), \quad (2)$$

$$\tilde{H}_{Re}(\xi,t) \equiv \mathcal{P}\int_0^1 dx\,\left[\tilde{H}(x,\xi,t) + \tilde{H}(-x,\xi,t)\right]C^-(x,\xi), \quad (3)$$

$$\tilde{E}_{Re}(\xi,t) \equiv \mathcal{P}\int_0^1 dx\,\left[\tilde{E}(x,\xi,t) + \tilde{E}(-x,\xi,t)\right]C^-(x,\xi), \quad (4)$$

$$H_{Im}(\xi,t) \equiv H(\xi,\xi,t) - H(-\xi,\xi,t), \quad (5)$$

$$E_{Im}(\xi,t) \equiv E(\xi,\xi,t) - E(-\xi,\xi,t), \quad (6)$$

$$\tilde{H}_{Im}(\xi,t) \equiv \tilde{H}(\xi,\xi,t) + \tilde{H}(-\xi,\xi,t), \quad (7)$$

$$\tilde{E}_{Im}(\xi,t) \equiv \tilde{E}(\xi,\xi,t) + \tilde{E}(-\xi,\xi,t), \quad (8)$$

with the coefficient functions $C^{\pm}$ being defined as:

$$C^{\pm}(x,\xi) = \frac{1}{x-\xi} \pm \frac{1}{x+\xi}. \quad (9)$$

We see that the CFFs depend only on ξ and t, not x. We restricted this work to 7 independent CFFs only, neglecting $\tilde{E}_{Im}$. Indeed, the $\tilde{E}$ CFF is commonly associated to the pion pole, a purely real function.

To reach a kinematical regime in which the virtual photon can probe quarks, the squared lepton 4-momentum transfer is typically larger than $\sim$1 GeV^2. We note this transfer, the photon's virtuality, Q^2=-q^2 for DVCS and Q'^2=+q'^2 for TCS, where q and q' are the 4-momenta of initial and final photons. Both DVCS and TCS processes interfer with Bethe-Heitler (BH) process. For DVCS, the associated BH process corresponds to the emission of a real photon from the lepton beam in the nucleon field (Fig. 3). For TCS, the associated BH process corresponds to the splitting of the incoming photon into a lepton pair in the nucleon field (Fig. 4).

The unpolarized DVCS+BH and TCS+BH processes depend on 5 independent variables. At QCD leading order and leading twist, their amplitudes are complex conjugate [1]. It is therefore possible to extract the same CFFs (up to a sign change for the imaginary part) at the same kinematic (ξ, t) point with the two reactions. Thus, we shall take ξ and t a two of the 5 independent variables for both reactions. For the DVCS+BH process, we take for the 3 additional variables the incoming photon virtuality (Q^2), the electron beam energy (E) and the azimuthal angle between the lepton scattering plane and the proton-final photon plane (ϕ). Fig. 5 (top panel) shows a scheme of the DVCS reaction. For the TCS+BH process, for the 3 variables other than ξ and t, we take the final photon virtuality (Q'^2) and the polar and azimuthal angles of the lepton pair (θ, ϕ) defined in after a boost the γ^* rest frame, as represented in Fig. 5 (bottom right panels). When the nucleon target is polarized transversely, DVCS+BH and TCS+BH depend in addition on the spin direction of the nucleon with respect to the reaction plane through an angle which we call ϕ_S. The TCS+BH process with a linearly polarized photon beam also depends on an additioanl variable, namely the orientation of the photon spin with respect to the reaction plane (Ψ_S). In the following, we generate ϕ distributions for various observables for both DVCS and TCS. For these distributions, we fix ξ and t values, so that the underlying CFFs are the same. We will try to recover, by fit, the

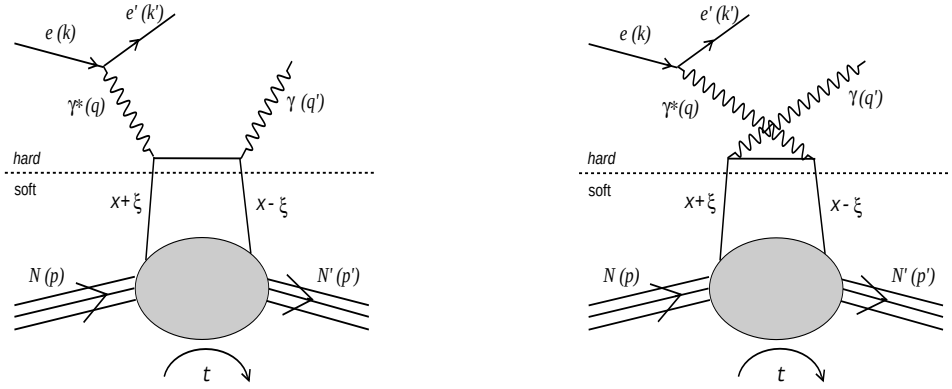

Figure 1: DVCS leading order and leading twist "handbag" diagrams.

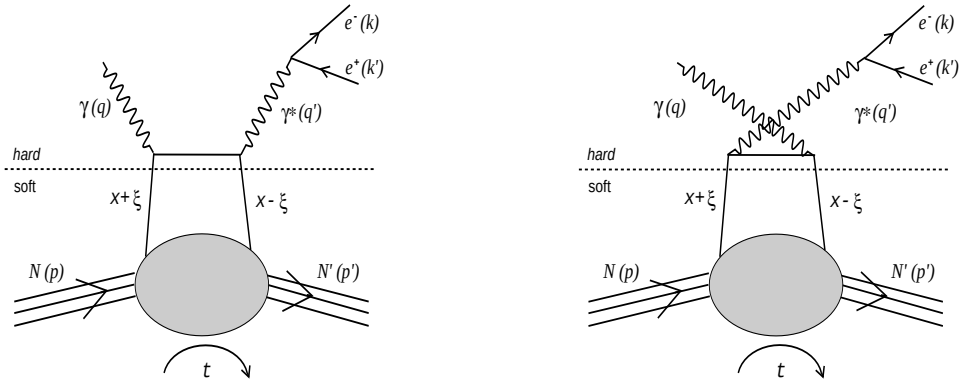

Figure 2: TCS leading order and leading twist "handbag" diagrams.

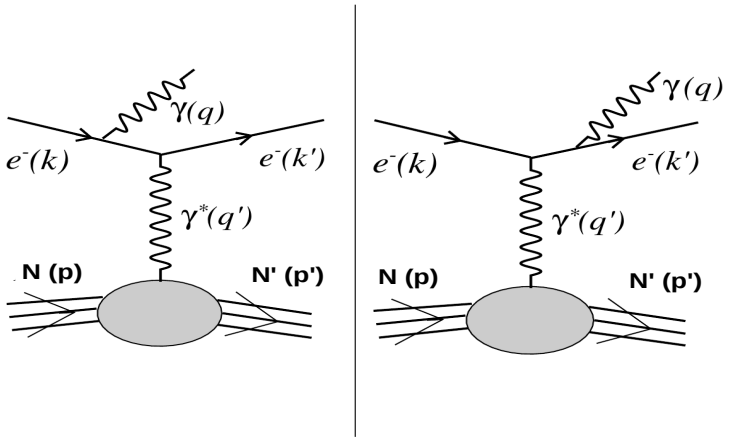

Figure 3: The Bethe-Heitler process interfering with DVCS.

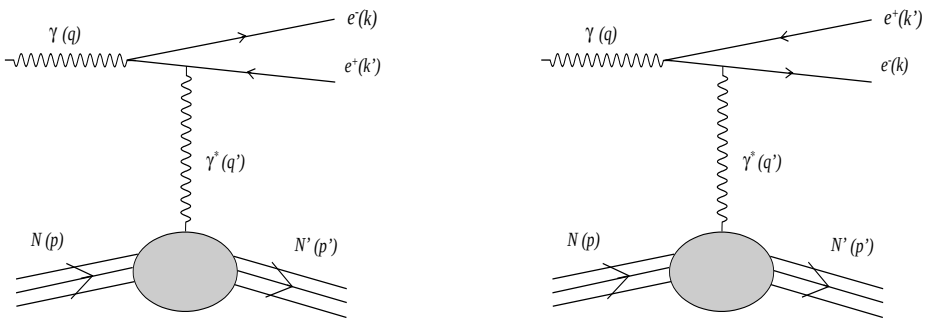

Figure 4: The Bethe-Heitler like process interfering with TCS.

originally generated CFFs. For the other variables, E, Q^2, Q'^2, θ, we took typical values accessible with JLab at 12 GeV. The general shapes of the ϕ distributions of DVCS+BH and TCS+BH is sin or cos(Nϕ) harmonics. Their magnitude depend on the relative weight of DVCS and TCS with respect to BH, which is function of the kinematics.

The potential to extract the same CFFs from DVCS and TCS allow for demonstrating GPDs universality, which is a milestone to prove QCD structure functions universality. It is possible at Jefferson Lab to carry out such comparison, as DVCS and TCS share some common phase space (Fig. 6). In addition, assuming GPD universality and neglecting QCD next to leading order and twist effects, extracting CFFs from DVCS and TCS simultaneously allow for bringing constraints to multiparameters CFF fits.

2 Observables and pseudo-data

We generated DVCS+BH and TCS+BH pseudo-data sets based on VGG model for GPDs [2, 3, 4, 5, 6], and using 7 independent CFFs as explained previously. The cross sections are calculated at a typical JLab kinematics, at same t and ξ for DVCS and TCS. We generated DVCS+BH distributions at: t=-0.2 GeV^2, $\xi = 0.15$, Q'^2 = 2.5 GeV^2, E(beam) = 11 GeV, We generated TCS+BH distributions at: t=-0.2 GeV^2, $\xi = 0.15$, Q^2 = 4.5 GeV^2, θ_{CM} = 90°. We did the calculations for 16 bins in ϕ. In case of transversally polarized proton, we generated the polarized cross sections at $\phi_S = 0°$ (spin along x-axis) and at $\phi_S = 90°$ (beam along y-axis). In case of TCS from a linearly polarized photon beam, we generated the polarized cross sections at $\Psi = 0°$ (spin in the reaction plane) and at $\Psi = 90\circ$ (spin transverse to the reaction plane).
We define the cross sections differences for DVCS with a longitudinaly polarized beam (electron) and for TCS with circularly polarized beam (photon), respectively as:

$$\Delta\sigma_{LU\,(\odot U)} = \frac{1}{2}[\sigma^{\rightarrow} - \sigma^{\leftarrow}], \tag{10}$$

where $\sigma^{\uparrow}$ and $\sigma^{\downarrow}$ correspond for DVCS+BH to a spin polarization vector aligned and anti-aligned along the lepton beam direction respectively. The arrows correspond for TCS+BH to left or right circularly polarized photons. The first index "L" for DVCS indicates that the lepton beam is longitudinaly polarized, the first index "$\odot$" (for TCS) indicates that the photon beam is circularly

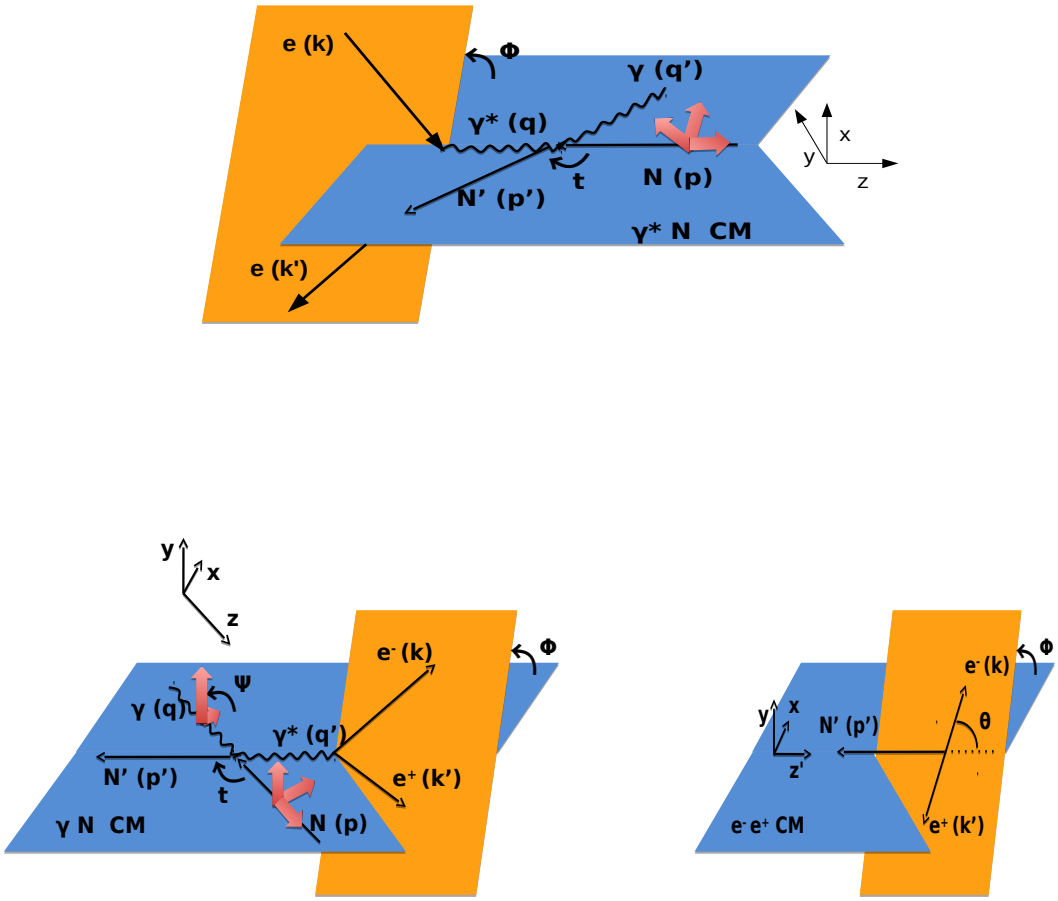

Figure 5: Top: scheme of DVCS reaction in $\gamma * N$ CM frame. Bottom: scheme of TCS reaction in γN and in γ^* CM frames. Reaction planes are colored in blue and leptonic planes in orange. 4-vectors notation of particles is indicated. Red arrows indicate possible polarizations for incoming particles. We indicated ϕ angles (same notation for DVCS and TCS) as the angle between the leptonic and the $\gamma\gamma*$ planes, and for TCS we indicated the θ angle between the final electron and the reaction plane after boost to γ^* CM frame. We noted Ψ for TCS the angle between the linearly polarized beam and the reaction plane.

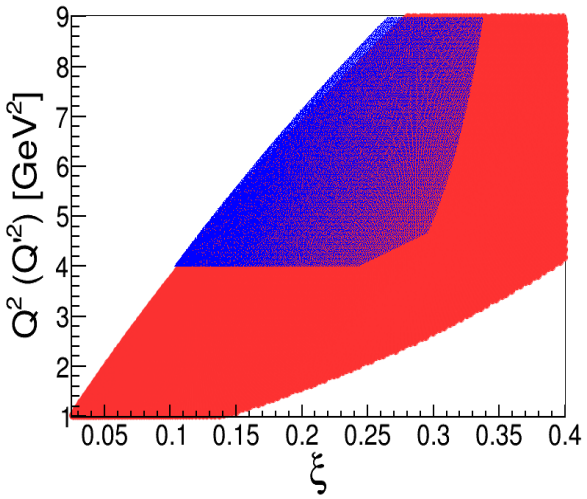

Figure 6: Phase space for DVCS+BH (in blue) and TCS+BH (in red) reactions as a function of ξ and Q^2 (Q'^2 for TCS). We assumed an electron beam energy of 11 GeV for DVCS and from 5 to 11 GeV for TCS, a maximal square transfer momentum -t< 1 GeV^2, and a proton-virtual photon energy cut of W> 2 GeV for DVCS. We limited the mass of the virtual photon of TCS as $4 < Q'^2 < 9$ GeV^2 to avoid interference with resonant states (limited by ρ' and J/Ψ masses).

polarized. The second index "U" indicates that the target is unpolarized.

Similarly, we define the linearly polarized target cross section difference as

$$\Delta\sigma_{UL} = \frac{1}{2}[\sigma^{\rightarrow} - \sigma^{\leftarrow}], \tag{11}$$

where the second index "L" indicates that the target is longitudinally polarized while the beam (first index) is unpolarized. We define the transversally polarized target cross section differences at fix ϕ_S as

$$\Delta\sigma_{UT}(\phi_S) = \frac{1}{2}[\sigma(\phi_S) - \sigma(\phi_S + \pi)]. \tag{12}$$

In the following, we fix the transverse target polarization along the x-axis ($\phi_S = 0°$) or along the y-axis ($\phi_S = 90°$).

We define the double beam and target spin cross section differences as

$$\Delta\sigma_{Li\,(\odot i)} = \frac{1}{4}[(\sigma^{\rightarrow\rightarrow} + \sigma^{\leftarrow\leftarrow}) - (\sigma^{\rightarrow\leftarrow} + \sigma^{\leftarrow\rightarrow})], \tag{13}$$

where the second index "i" indicates the polarization axis of the target (x, y, z, or any other transverse direction). Uppercase arrows on cross sections indicate the direction of the beam polarization and the target polarization, respectively.

We defined the TCS+BH linearly polarized beam cross section difference at fix Ψ_S as

$$\Delta\sigma_{LU}(\Psi_S) = \frac{1}{2}[\sigma(\Psi_S) - \sigma(\Psi_S + \frac{\pi}{2}]. \tag{14}$$

We defined the DVCS beam charge asymmetries (originating from an electron or positron beam) as

$$\Delta\sigma_C = \frac{1}{2}[\sigma(e^+) - \sigma(e^-)]. \quad (15)$$

All the distributions that we generated and used for extracting the CFFs in this note are shown on Fig. 7 (DVCS+BH) and Fig. 8 (TCS+BH).

3 CFF extraction method

We extracted the CFFs according to the fitting method from [7] from the various sets of the pseudo-data observables that we generated. In order to match the uncertainties expected in short term experiments at JLab, and to compare DVCS and TCS in the same conditions, we set relative errors of 5% per bin in ϕ for both DVCS+BH and TCS+BH unpolarized cross sections. We set relative errors of 7% per bin in ϕ for all the polarized cross sections. The free parameters of the fits are the 7 Compton Form Factors: $\Im(\mathcal{H})$, $\Im(\tilde{\mathcal{H}})$, $\Im(\mathcal{E})$, $\Re(\mathcal{H})$, $\Re(\tilde{\mathcal{H}})$, $\Re(\mathcal{E})$, $\Re(\tilde{\mathcal{E}})$. Rather than directly fitting the CFF, we extract coefficients of the generated CFFs values, which are set to 1 when the generated value is recovered. We limit the variation of all the coefficients during the minimization procedure to stay in a range of $[-5, +5]$, in order to force underconstrained fits to converge. The impact of limitating the variation of the coefficients on uncertainties and on correlation between the extracted CFFs is discussed in [8]. The fits are initiated to start all coefficient variation at a random number within the $[-5, +5]$ limits. As shown on Fig. 9, the result of the fit (mean value) has a dependence on the starting point and fluctuate around the generated value. However, the $\pm 1\sigma$ limits of the result are stable. To check if CFFs can be extracted from actual data, we also smear the generated cross section points within 1σ of the uncertainties. Similarly, we started the fits from random values of the coefficients. We obtained broader distributions of the results and their limits, with a resolution including the uncertainties on the observables and the correlation between the different CFFs (Fig. 10).

We fitted the results of the fits (CFF value and 1σ errors) by gaus functions. When a given CFF can be extracted from a specific set of observables, we found stable results and allocated the fitted 1σ limits as uncertainties on extracted CFFs. To avoid overcounting the uncertainties on CFFs and in our goal of comparating DVCS and TCS, we used the unsmeared distributions of pseudo-data for this exercise.

In some cases of underconstrained fits, we obtain two sets of extracted CFF coefficients as two solutions can minimize the problem. I correspond to cases where not all CFFs can be extracted at the same time. One of the solution correspond to a "good" and stable extraction of the generated CFFs. The other solution correspond to cases where one or several parameter reach one of its variation limits. Because of the correlation between the CFFs, wrong values of other CFFs are extracted. This solution is easily rejected by variating the limits of the parameters.

4 Results

We performed fits on the sets of observables presented on table 1. For configurations 1 to 5, we systematically performed fits for DVCS and TCS independently, and combining both reactions. For the configurations 6, 6', 6", we fitted observables from DVCS, TCS, DVCS+TCS, respectively (the symbol "x" in the table indicate configurations that are not fitted). In the table we used the

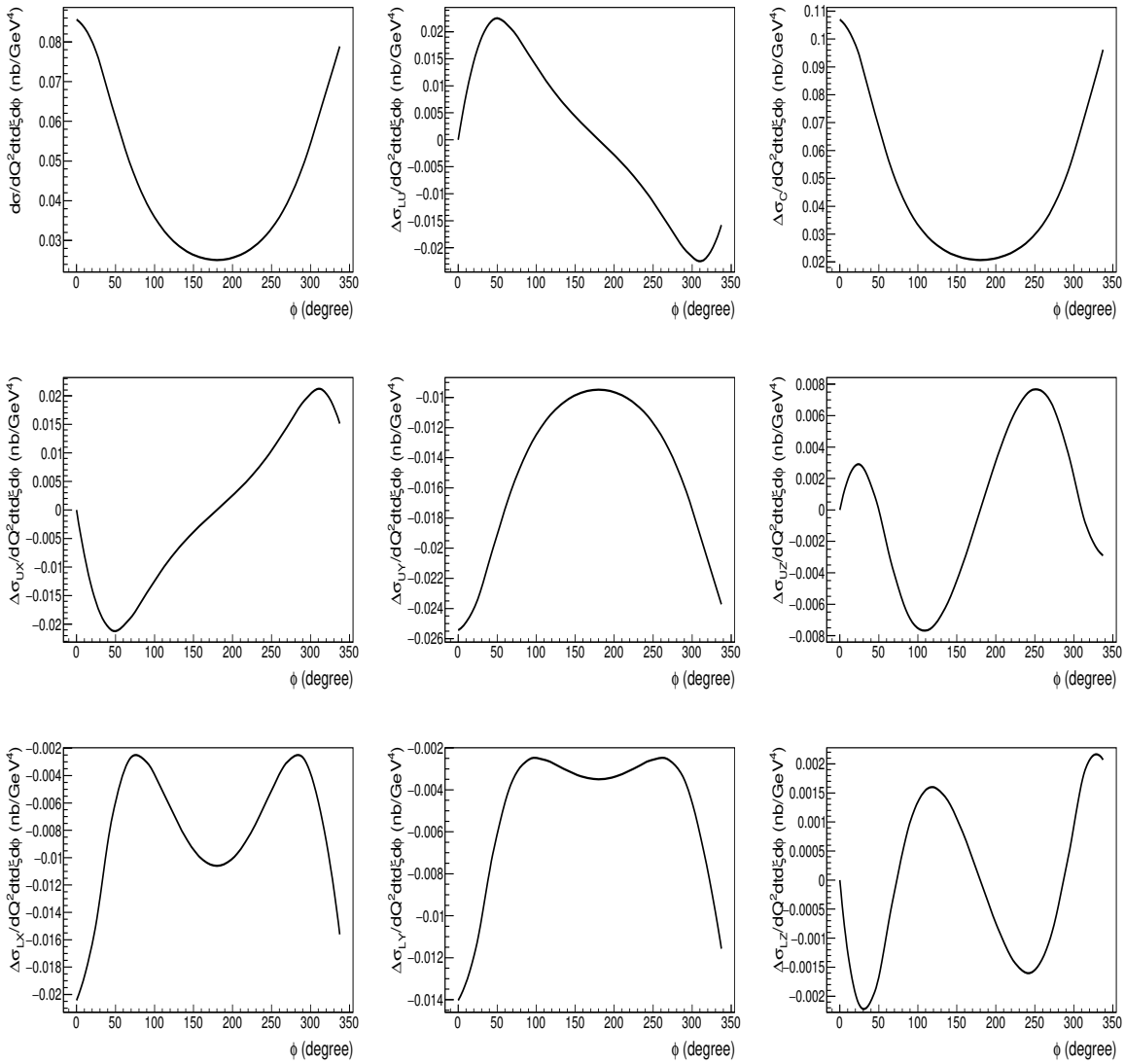

Figure 7: Generated distributions for DVCS+BH process. First row: unpolarized cross section (left), beam spin cross section differences (center), beam charge cross section differences (right). Second row: target spin cross section differences with the target spin along x-axis (left), y-axis (center), z-axis (right). Third row: double spin cross section differences with a longitudinally polarized electron and with the target spin along x-axis (left), y-axis (center), z-axis (right). The cross sections are calculated for $\xi = 0.15$, -t = 0.2 GeV^2, Q^2 = 2.5 GeV^2, E(e$^-$)= 11 GeV.

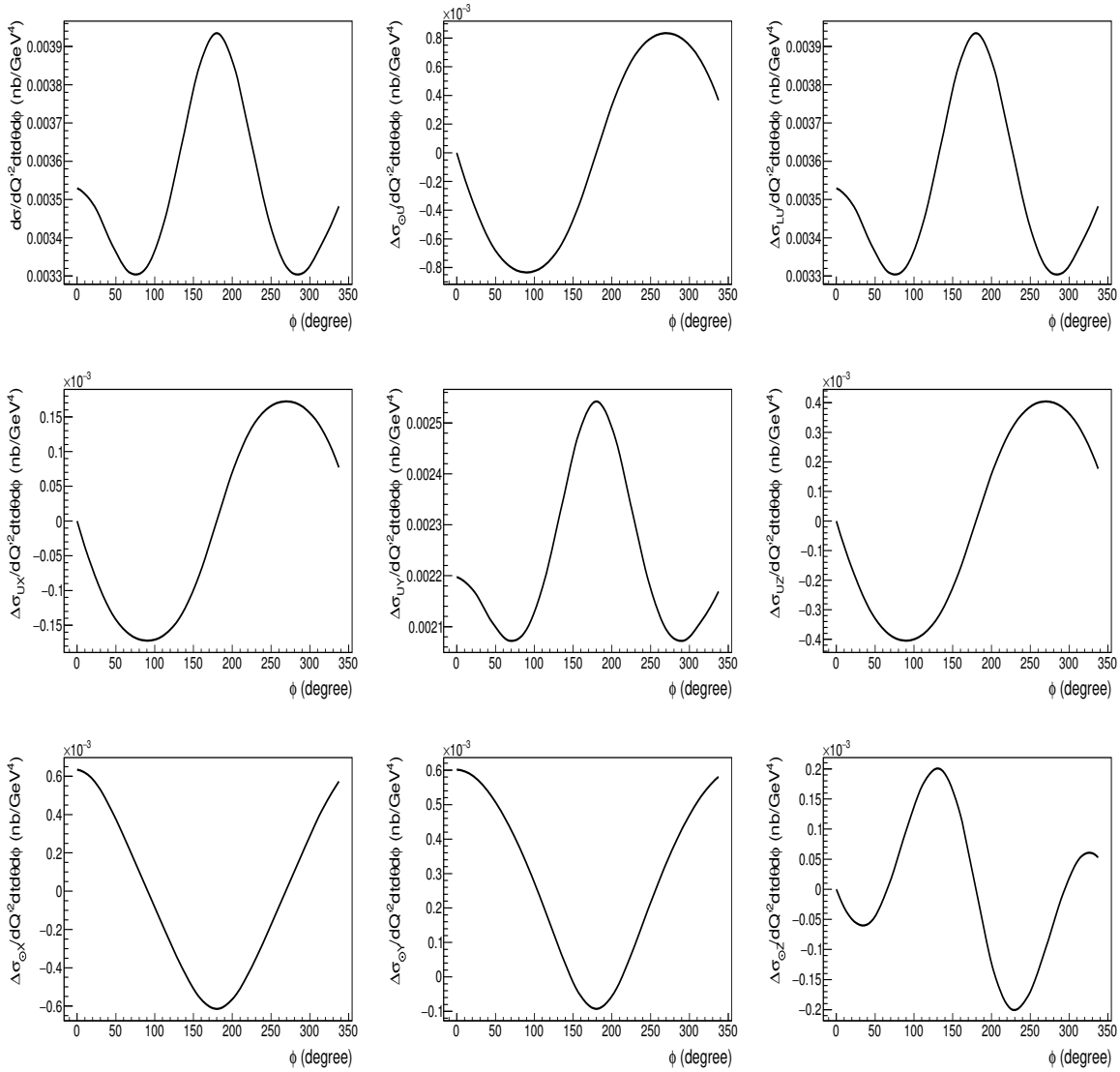

Figure 8: Generated distributions for TCS+BH process. First row: unpolarized cross section (left), beam spin cross section differences (center = circularly polarized beam, right = linearly polarized beam). Second row: target spin cross section differences, with the target spin along x-axis (left), y-axis (center), z-axis (right). Third row: double spin cross section differences, with a circularly polarized photon and with the target spin along x-axis (left), y-axis (center), z-axis (right). The cross sections are calculated for $\xi = 0.15$, -t = 0.2 GeV^2, Q$'^2$ = 4.5 GeV^2 and $\theta = 90^\circ$.

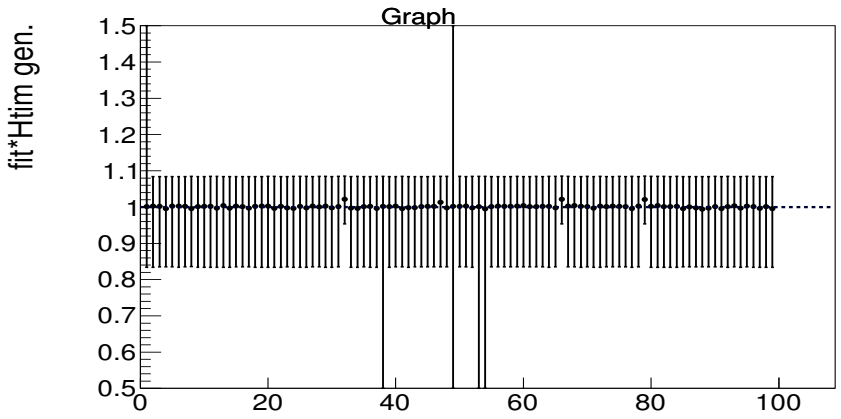

Figure 9: Result for $\Im\tilde{\mathcal{H}}$ of fitting 100 time the same distribution starting from a random value for all CFF coefficients in $[-5, +5]$. We fitted simultenaously DVCS+BH unpolarized cross section, beam spin and longidutinal target single and double polarized cross section differences.

notations corresponding to DVCS observables: the first index "L" for designing beam spin asymmetries should be replace by an index "$\odot$" in case of TCS (circularly polarized beam).

Set of observables	DVCS	TCS	DVCS+TCS	# independent obs. (DVCS/TCS/both)
1) σ, $\Delta\sigma_{LU}$	A, B, C	A, B, C	A, B, C	2/2/2
2) σ, $\Delta\sigma_{LU}$, $\Delta\sigma_{UL}$, $\Delta\sigma_{LL}$	B	-	-	4/4/4
3) σ, $\Delta\sigma_{LU}$, $\Delta\sigma_{UT}$ (x2)	-	C	-	4/4/4
4) σ, $\Delta\sigma_{LU}$, $\Delta\sigma_{UT}$ (x2) $\Delta\sigma_{UL}$, $\Delta\sigma_{LL}$	-	-	-	6/6/6
5) σ, $\Delta\sigma_{LU}$, $\Delta\sigma_{UT}$ (x2) $\Delta\sigma_{UL}$, $\Delta\sigma_{LL}$, $\Delta\sigma_{LT}$ (x2)	-	-	-	8/8/8
6) σ, $\Delta\sigma_{LU}$, $\Delta\sigma_{C}$	-	x	x	3 (DVCS)
6') σ, $\Delta\sigma_{\odot U}$, $\Delta\sigma_{LU}$	x	D	x	3 (TCS)
6") 2) of DVCS + 3) of TCS	x	x	B+C	6 (DVCS+TCS)

Table 1: First column: set of combined observables for DVCS, TCS and DVCS+TCS fitting. Second to fourth column: current and future experiments at JLab accessing these observables (letters indicate experimental Halls). Fifth column: number of uncorrelated observables.

The first 3 data sets correspond to measurements planned in a short term at JLab. We indicated by the letter the experimental Hall which can perform the measurement. When no expected experiment corresponds to the presented configuration, we indicate it by a symbol "-". Running or

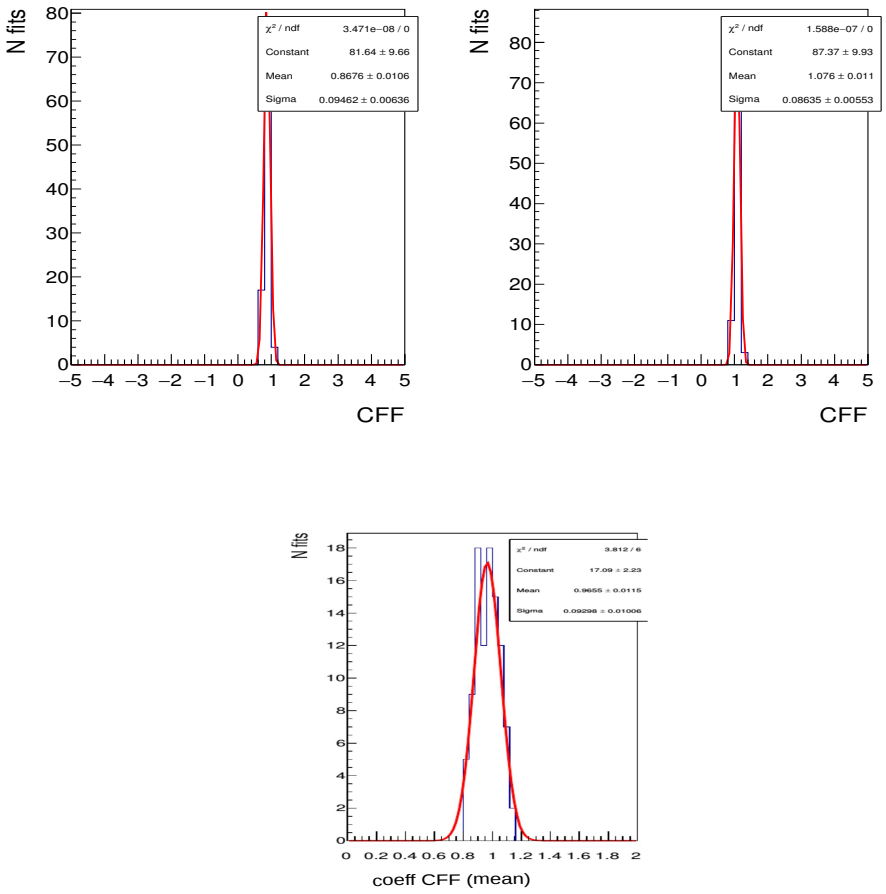

Figure 10: Top: Minimal (left) and maximal (right) limits of $\Im\tilde{\mathcal{H}}$ extracted from fitting 100 times smeared distributions of the same observables, and starting from a random value for all CFF coefficients in $[-5, +5]$. Bottom: fit result (central value) for the same distributions. We fitted simultenaously DVCS+BH unpolarized cross section, beam spin and longidutinal target single and double polarized cross section differences.

approved experiments at JLab (12 GeV) include the experiments [9, 10, 11] aiming at measuring the unpolarized and beam polarized DVCS cross sections, the experiment [10] will also measure the longitudinally polarized target single and double spin asymmetries, and the conditionally approved experiment [12] aims at measuring the transverse target spin asymmetries. Complementary TCS experiments at JLab (12 GeV) include the experiments [13] (running) and [14] (future) aiming at measuring the unpolarized and circularly beam polarized cross section of TCS, from a quasi-real photon beam (the incoming beam is a longitudinally polarized 11 GeV electron). Another project aims at measuring the TCS transverse target asymmetries in addition to the unpolarized and circularly polarized photon beam cross sections [15]. The 5^{th} data set is an ideal case where all spin configurations can be measured simultenaously. Since fits are overconstrained in this case (8 independent observables), it represent the ideal uncertainties on CFFs reachable for given experimental uncertainties. The extracted CFF uncertainties are presented on Fig. 11 (imaginary parts) and 12 (real parts).

4.1 Interpretation on fitting DVCS or TCS independently

Measuring only the unpolarized cross section and beam spin asymmetry either from DVCS+BH or from TCS+BH (with a circularly polarized beam for TCS) allow for extracting $\Im\mathcal{H}$, $\Im\tilde{\mathcal{H}}$, and $\Re\mathcal{H}$ with a good enough precision for contributing in constraining GPD models. Having in addition the longitudinal target spin asymmetry allow for constraining better these CFFs, in particular $\Im\tilde{\mathcal{H}}$, and allow for bringing some constraints on $\Re\tilde{\mathcal{H}}$.

Having in addition to the unpolarized cross section and beam spin asymmetry two independent transverse target spin asymmetry allow to constrain in addition $\Im\mathcal{E}$. Thanks to the correlations between CFFs and the fact of having more independent observables to constrain the fits, a much better precision is reached for $\Re\mathcal{H}$ compared to cases without transverse target asymmetries.

Fitting DVCS+BH or TCS+BH unpolarized cross sections, beam polarized cross sections, 3 single target polarized cross sections (1 longitudinnal, 2 transverse), and the double beam and longitudinaly target polarized cross section bring constraint to $\Im\mathcal{H}$, $\Im\tilde{\mathcal{H}}$, $\Im\mathcal{E}$, $\Re\mathcal{H}$, $\Re\tilde{\mathcal{H}}$ and $\Re\mathcal{E}$. Adding the double beam and transverse target spin asymmetries will strongly shrink the uncertainties for all the CFFs and avoid incorrect solutions to the problem, thanks to it being overconstrained. The CFF $\Re\tilde{\mathcal{E}}$ is constraint thanks to correlations with other CFFs.

We notice that in a scenario of same uncertainties on DVCS and TCS observables, the sensitivities to CFFs of DVCS observables are stronger the sensitivities of TCS observables. Indeed, TCS is more suppressed than DVCS compared to the associated BH process. However, we can constrain CFFs from the two reactions independently and compare the results to demonstrate GPDs universality. We also notice that for both reactions we are more sensitive to the imaginary part of the amplitudes than the real parts: BH contribution to single spin asymmetries, sensitive to imaginary part of the amplitudes (except for the linearly polarized beam TCS), doesn't cancel. As a consequence, the sensitivity to CFFs is limited to the difference between the asymmetry induced by the BH process and the asymmetry coming from the interference between DVCS and BH (respectively TCS and BH). We found a weak impact in the results for extracted CFFs of measuring the linearly polarized TCS cross sections or the DVCS beam charge asymmetries, which are sensitive to real part of amplitudes. The reason is that the contribution of CFFs to the total cross section is low, as well as differences coming from the parametrization, due to the large dominance of BH. However,

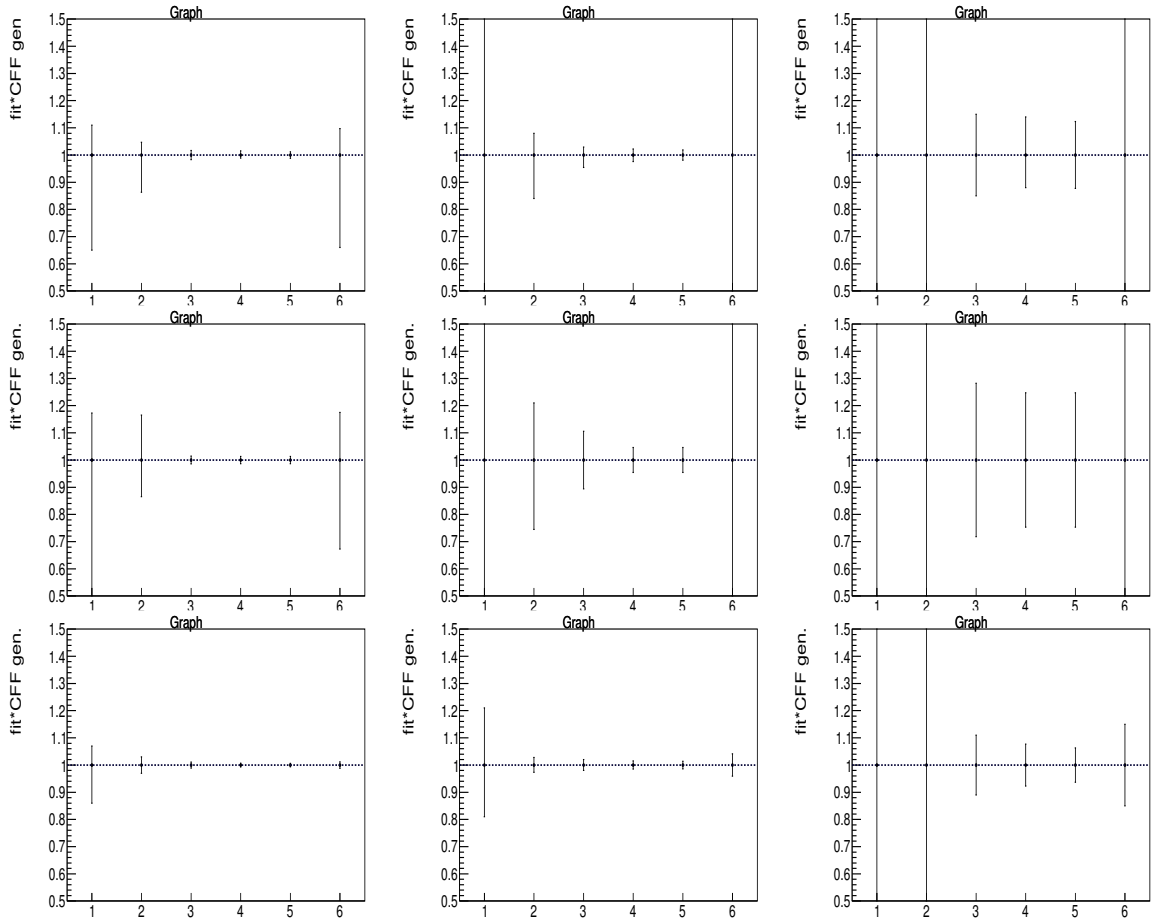

Figure 11: Extracted coefficients for imaginary part of CFFs, defined as fit result * generated CFF. Left column: Im($\mathcal{H}$), central column: Im($\tilde{\mathcal{H}}$), right column: Im($\mathcal{E}$). Top: extracted from DVCS, central row: extracted from TCS, bottom row: extracted from DVCS+TCS. Set of observable indices (from 1 to 6) are detailed in table 1. The scale is zoomed, fitting coefficient variation has been limited to $[-5, 5]$ time the generated one. Generated coefficient (1) is indicated by the black dashed line.

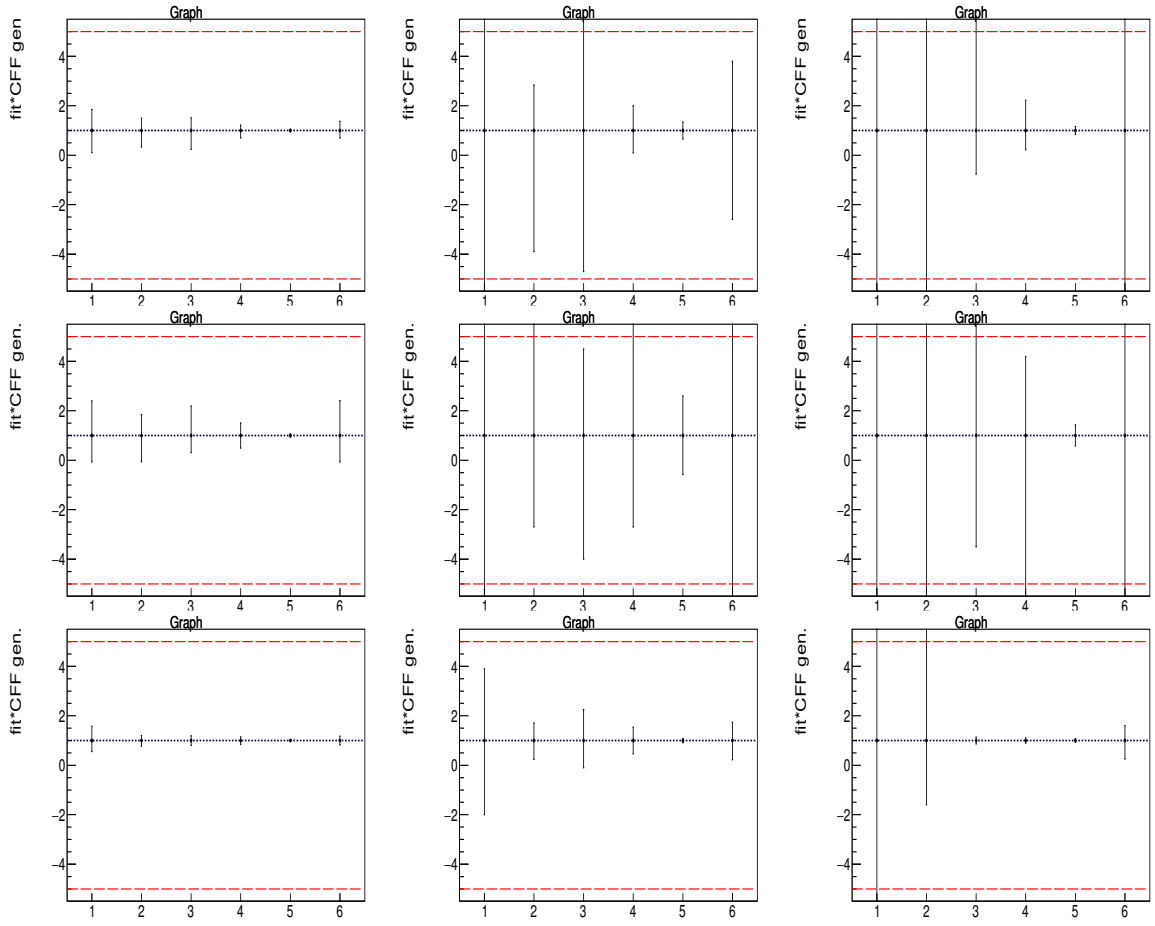

Figure 12: Extracted coefficients for real part of CFFs, defined as fit result * generated CFF. Left column: Re($\mathcal{H}$), central column: Re($\tilde{\mathcal{H}}$), right column: Re($\mathcal{E}$). Top: extracted from DVCS, central row: extracted from TCS, bottom row: extracted from DVCS+TCS. Set of observable indices (from 1 to 6) are detailed in table 1. Fitting coefficient variation has been limited to $[-5, 5]$ times the generated one. These limits are indicated by the red dashed lines. Generated coefficient (1) is indicated by the black dashed line.

with a significantly better statistic precision, these two observables could bring strong constraint to the real part of amplitudes.

4.2 Interpretation on fitting simulteanously DVCS and TCS

In the first 5 data sets, we fitted simulteanously correlated observables from DVCS and from TCS. These simultenaous fits allow for about a factor of 2 reduction of error bars compared to the case of fitting only DVCS. This reduction is larger than statistically expected, due to the fact that the unpolarized cross sections are not fully correlated and therefore they bring some new information. Combining observables from both reactions can help at a non negligible level in constraining GPD models by reducing uncertainty and allowing for extraction of CFFs which would be hard to constraint otherwise.

The 6" data set is a combination of DVCS 2^d data set and TCS 3^d data set, corresponding to short term approved or proposed experiments at JLab. Independent information is brought by the different target polarization accessible in these experiments. Combining these data sets allow for constraining at the same time all CFFs.

Even thought simultenaous fits are assuming GPDs universality, they allow for bringing strong constraint to GPD models with short term upcoming DVCS and TCS experiments. Next to leading twist and next to leading order are not taken into account in this picture and may enlarge the error bars on extracted CFFs from simultaneous fits. Combined fits and comparison of DVCS and TCS results will also help understanding higher order effect in the two reactions.

5 Conclusion

We presented in this note our results for DVCS, TCS and combined DVCS and TCS fits for CFFs extraction. We discussed the impact on constraning several CFFs and GPD models from short and longer term measurements at JLab. Fitting independently set of observables from DVCS and TCS allow for demonstrating GPDs universality, assuming that we can neglect higher twist effects and NLO contributions. Under this assumption, we can combined data sets from the two reactions for better constraining CFFs. In this approach, a large number of independent observables is needed for extracting all CFFs at the same time and simultenaous fits allow for improving knowledge on GPDs with short term planned experiments. It has however been shown in recent DVCS measurements that higher twist effects are non negligible [16]. Comparing results from DVCS and TCS can allow for an estimation.

References

[1] M. Diehl, Phys. Rept. **388** (2003) 41

[2] Vanderhaeghen M, Guichon P A M and Guidal M 1998 *Phys. Rev. Lett.* **80** 5064

[3] M. Vanderhaeghen, P. A. M. Guichon and M. Guidal, Phys. Rev. D **60** (1999) 094017 doi:10.1103/PhysRevD.60.094017

[4] Guidal M, Polyakov M V, Radyushkin A V and Vanderhaeghen M 2005 *Phys. Rev. D* **72** 054013

[5] Goeke K, Polyakov M V and Vanderhaeghen M 2001 *Prog. Part. Nucl. Phys.* **47** 401

[6] M. Boër, M. Guidal and M. Vanderhaeghen, Eur. Phys. J. A **51** (2015) no.8, 103.

[7] Guidal M 2008 *Eur. Phys. J. A* **37**, 319 [Erratum-ibid. A **40**, 119 (2009)]

[8] M. Boër and M. Guidal, J. Phys. G **42** (2015) no.3, 034023

[9] C. Hyde-Wright, B. Michel, C. Munoz Camacho and J. Roche, JLab experiment E12- 06-114.

[10] F. Sabatié, A. Biselli, V. Burkert, L. Elouadrhiri, M. Garçon, M. Holtrop, D. Ireland, K. Joo, W. Kim, JLab experiment E12-06-119.

[11] C. Munoz Camacho, R. Paremuzyan, T. Horn, JLab experiment E12-13-010.

[12] L. Elouadrhiri, H. Avakian, V. Burkert, M. Guidal, M. Lowry, L. Pappalardo, and S. Procureur, JLab experiment E-12-12-010, conditionally approved.

[13] JLab experiment E12-12-001: Timelike Compton Scattering and J/ψ photoproduction on the proton in e^+e^- pair production with CLAS12 at 11 GeV.

[14] JLab experiment E12-15-006A: Timelike Compton Scattering with SoLID, run group proposal to the PAC 43 (2015).

[15] M. Boer, V. Tadevosyan, Experimental project at the JLab Hall C: Timelike Compton Scattering off transversely polarized proton, to be submitted (2018).

[16] M. Defurne *et al.* [Jefferson Lab Hall A Collaboration], Phys. Rev. C **92** (2015) no.